

See discussions, stats, and author profiles for this publication at: <https://www.researchgate.net/publication/291344992>

Sensorless field oriented control of BLDC motors for MAVS

Article in Transactions on Electrical Engineering · December 2015

CITATIONS

9

READS

2,811

4 authors, including:



Dávid Rau

Slovak University of Technology in Bratislava

3 PUBLICATIONS 19 CITATIONS

[SEE PROFILE](#)



Jozef Rodina

Slovak University of Technology in Bratislava

22 PUBLICATIONS 71 CITATIONS

[SEE PROFILE](#)



Peter Hubinský

Slovak University of Technology in Bratislava

73 PUBLICATIONS 269 CITATIONS

[SEE PROFILE](#)

Some of the authors of this publication are also working on these related projects:



Innovative HRI methods for robots' control in the real environment [View project](#)



A Network of Robotics DIHs for Agile Production [View project](#)

Sensorless Field Oriented Control of BLDC Motors for MAVs

Dávid Rau ¹⁾, Jozef Rodina ²⁾, Lukáš Palkovič ³⁾ and Peter Hubinský ⁴⁾

¹⁾ Institute of Robotics and Cybernetics, Bratislava, Slovakia, e-mail: david.rau@stuba.sk

²⁾ Institute of Robotics and Cybernetics, Bratislava, Slovakia, e-mail: jozef.rodina@stuba.sk

³⁾ Institute of Robotics and Cybernetics, Bratislava, Slovakia, e-mail: palkovic.lukas@gmail.com

⁴⁾ Institute of Robotics and Cybernetics, Bratislava, Slovakia, e-mail: peter.hubinsky@stuba.sk

Abstract — To achieve longer flight duration of the micro aerial vehicles (MAVs) it is needed to optimize their propulsion system. A typical propulsion system of VTOL (vertical take-off and landing) MAV consist of the propeller BLDC (brushless DC) motor, motor controller and battery (typically Lithium based chemistry). All these parts of the propulsion system can be optimized in a specific way. In the case of the propeller, this can be done by the optimization of static and dynamic thrust performance. The motor construction can be optimized by using lighter materials or stronger rotor magnets. As for the battery - alternative power sources like solar panels, hydrogen fuel cells etc. may be used. We are focusing on the optimization of the motor control part. In this paper, we are presenting synthesis of the BLDC controller using the field oriented control strategy which promises better performance in the dynamical response of the propulsion system, lower power consumption and generally higher efficiency in comparison with the traditional six step commutation techniques.

Keywords — MAV, BLDC, FOC, vector control, observer.

I. INTRODUCTION

Growth of the micro aerial vehicle market brings a new application which requires more sophisticated and advanced MAVs. The most often named requirement for such type of vehicle is longer flight duration. There are several solutions/studies how to increase the flight duration, for instance by using hydrogen fuel cells [1], by using solar cells [2] etc. Most of these projects are concentrating on the usage of alternate power sources instead of classical Lithium chemistry based batteries. But there is also another way of how to increase the flight length and it is by optimizing the propulsion system itself. In the case of copter type MAVs we can optimize the used propeller, motor and motor controller. Mostly used motor types are the BLDC which are controlled using six step commutation strategy with the BEMF zero crossing detection [3]. The pros of this technique are cheap HW and FW and also the fact that there is no real need to have motor parameters like stator inductance, nor resistance to be able to start the rotation with motor. The cons of this approach are not an ideal dynamical behaviour when higher dynamical response of the motor control is needed and also that the efficiency of this approach is far from ideal. On the other side, a more advanced approach for controlling the three phase PMSM/BLDC motors is the field-oriented control (FOC) technique which can bring higher efficiency, higher dynamical response of the motor control and overall a better performance than the six step

commutation. However, this approach means also higher HW and FW costs. Nevertheless, even if the costs of HW and FW are higher, the usage of the FOC may lead to cost saves in professional applications of MAVs due to better performance. In this paper, we are presenting the FOC controller design for the BLDC motors in the Matlab SimPowerSystems.

II. MODEL OF MOTOR

A. Sim Power System Model

The simulation model of the brushless direct current (BLDC) motor is based on simulation blocks of the SimPowerSystems Toolbox in Simulink. For our purpose a simulation block called Permanent Magnet Synchronous Machine is used. This machine block based on a three-phase system can be applied like motor operating mode, as well as generator operating mode. The motor operating mode in our research is achieved by zero or positive values of the load torque brought to the model. In order to create a nonlinear model corresponding with to the real BLDC motor, it is necessary to set the outcome of the back electromotive force to a trapezoidal output. The output shape of the BEMF is caused by the salient motor structure. The electrical part of the motor model from the toolbox is defined at [1] by the following equations:

$$\frac{d}{dt}i_a = \frac{1}{3L_s} \left(2v_{ab} + v_{bc} - 3R_s i_a + \lambda p \omega_m (-2\phi'_a + \phi'_b + \phi'_c) \right) \quad (1)$$

$$\frac{d}{dt}i_b = \frac{1}{3L_s} \left(2v_{ab} + v_{bc} - 3R_s i_b + \lambda p \omega_m (-2\phi'_b + \phi'_a + \phi'_c) \right) \quad (2)$$

$$\frac{d}{dt}i_c = - \left(\frac{d}{dt}i_a + \frac{d}{dt}i_b \right) \quad (3)$$

$$T_e = p\lambda(\phi'_a \cdot i_a + \phi'_b \cdot i_b + \phi'_c \cdot i_c) \quad (4)$$

where i_x is the phase current, Φ'_x is the electromotive force, v_{xy} is the phase to phase voltage, L_s is the stator inductance, R_s is the stator resistance, λ is the flux of a permanent magnet, p represents the number of pole pairs, ω_m represents the angular velocity of the rotor and T_e the electromagnetic torque.

B. Simplified Model

The previous model is applicable for the verification of the motor behaviour, however, for the purpose of the control design it is necessary to simplify it. In this case,

the previous model has to be reduced to a linear model. The control design is based on the assumption that the control will be applied at a higher speed. In this case, the shape of the BEMF approaches a sinewave. By the means of the above mentioned simplification, it is possible to transform the BEMF into a DC value and therefore we can use a DC model shown in the following figure instead.

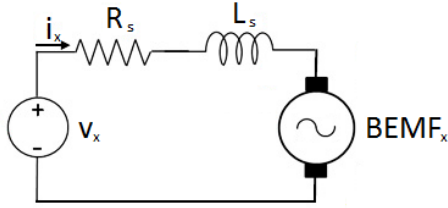


Fig. 1. Simplified model of the motor.

This model of the motor is described by transfer function $M(s)$ as follows

$$M(s) = \frac{U(s)}{I(s)} = \frac{\frac{1}{R_s}}{(1 + \frac{L_s}{R_s}s)} \quad (5)$$

In this case, the BEMF does not figure in the transfer function at (5) since it behaves as a constant with regards to the current and it does not influence the transient effect of the motor.

III. CONTROL

In order to control the entire drive, we applied the FOC of the BLDC motor using a simplified model of the motor from the previous chapter. For the FOC, the Clarke transformation was used in order to adjust the motor into a two-phase system and the Park transformation to change the stator reference frame into a rotor reference frame. By the above mentioned transformations, we have achieved the transformation of AC values to DC values of quantities, representing a prerequisite for the design of the control. These DC quantities allow designing a two level control – cascade control. The cascade control is necessary in order to apply the Maximum Torque per Ampere (MTPA) control described in [10]. The basic condition of the MTPA control is the achievement of an angle equal to ninety degrees between the rotor flux vector and the stator current vector. Since it is only the current that we can control, we need to use a cascade control with a current loop.

A. Current Loop

The low level control represents the current controllers. At this level, we control the amplitude and the angle of the current vector. The current vector is divided into the direct (I_d) and the quadrature (I_q) components of the current. These components of the current have to be regulated by maintaining the angle between the rotor flux and flow. We reached the angle of ninety degrees when the quadrature component reached the desired value – zero. In this case, the direct component affects only the size of torque.

The control loop comprises a PI controller and the above mentioned simplified model of the motor in (5). Closing this loop, we will get the $G(s)$ transfer function illustrated in (6) where K_a represents the proportional gain of the controller and K_b is the integral gain.

$$G(s) = \frac{(1 + \frac{s}{K_b})}{(\frac{L_s}{K_a K_b})s^2 + (\frac{R_s}{K_a K_b} + \frac{1}{K_a})s + 1} \quad (6)$$

The given transfer function contains two poles and one zero. Therefore, it is necessary to eliminate the zero from the numerator. Now we proceeded in accordance with [4]. We have split the denominator into two roots, focusing on the linear coefficient of the polynomial.

$$G(s) = \frac{(1 + \frac{s}{K_b})}{(1 + \frac{R_s}{K_a K_b}s)(1 + \frac{s}{K_b})} \quad (7)$$

By this arrangement in (7), we can eliminate the zero. Nevertheless, we have to fulfill all conditions – this means that the quadratic coefficient of the polynomial must be the product of roots. As a result of the fulfillment of the conditions, we have obtained one of the controller parameters.

$$K_b = \frac{R_s}{L_s} \quad (8)$$

In order to get the second parameter, it is necessary to substitute (8) into (7). By the above mentioned substitution we have obtained the transfer function of first order from [4] which depends on the bandwidth of the motor.

$$G(s) = \frac{1}{\frac{L_s}{K_a}s + 1} \Rightarrow K_a = L_s \cdot \text{Bandwidth}(\text{rad/s}) \quad (9)$$

By analysis, we obtained the parameters of the controller which are identical for both the direct and the quadrature components of the current.

B. Speed Loop

The higher level of the control represents the speed controller. The output of the controller is the desired torque which has to be transformed via the motor constant to the desired current in (10).

$$Mtr(s) = \frac{3}{2} \frac{P}{2} \lambda_r \quad (10)$$

This desired current is considered as an input of the quadrature current controller. Since we want to transform the entire current vector to torque, the set value of the direct current controller has to be zero. Based on these assumptions, we have created a closed speed loop as follows

$$GH(s) = \left(\frac{K_c K_d (1 + \frac{s}{K_d})}{s} \right) \left(\frac{1}{\frac{L_s}{K_a}s + 1} \right) \left(\frac{3}{4} P \lambda_r \right) \left(\frac{1}{k_v (\frac{J}{k_v}s + 1)} \right) \left(\frac{1}{\tau s + 1} \right) \quad (11)$$

where K_c represents the proportional gain of the controller, K_d is the integral gain of the controller, J is the moment of inertia and k_v is the viscous damping. We also applied a first order filter as a sensor of speed with time constant τ . In order to obtain the parameters of the speed controller, the method published in [5] and [6] was applied in the above mentioned transfer function as follows

$$K_c = \frac{1}{\delta K \tau} \quad (12)$$

$$K_d = \frac{1}{\delta^2 \tau} \quad (13)$$

where δ is the damping factor and K is the motor constant divided by the moment of inertia.

We are aware that the publication of the proposition management is not optimal. However, we decided to apply the solution because it comes from the successful application of the real product. Subsequent identification of motors is problematic and inaccurate. Therefore, we will surely find a place later the usage of adaptive control.

IV. OBSERVER

For the need of the sensorless BLDC motor control, it is necessary to create an observer of the feedback quantities. In our case, it is also necessary to know the angle of the rotor for the Clark transformation and the angular speed of the rotor for speed control.

A. Our Estimation

For the estimation of quantities, a system consisting of the BEMF observer and an element for estimate phase of the BEMF which is equal to the rotor angle was applied. Operates either in the stator reference frame, therefore the angle can be obtained as a result of a trigonometry function.

B. BEMF Observer

The BEMF observer can be designed using the simplified model of the motor. The actual measured current is considered as the disturbance which is compared with the current from the model. This error represents the input of the PI controller, the output of which is our desired BEMF as it is depicted in Fig. 2.

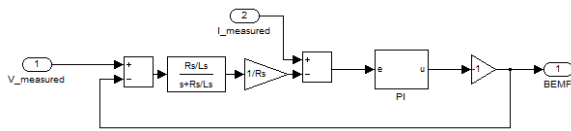


Fig. 2. BEMF observer based on the simplified model.

The second option is to use a state model of the motor where currents are compared as in the previous observer but difference of currents is multiplied by only the matrix L (P controller). In this case, the BEMF is not the output of the diagram but it is an internal variable. This process is shown in Fig. 3.

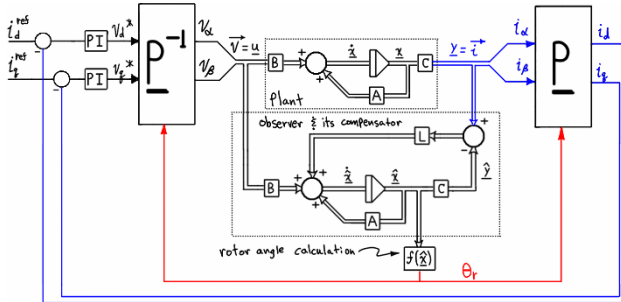


Fig. 3. State-space model of the BEMF observer [7].

Then the states x , output y , input u and matrices A , B , C may be written in accordance with [7] as follows

$$x = \begin{bmatrix} i_\alpha \\ i_\beta \\ e_\alpha \\ e_\beta \end{bmatrix} \quad y = \begin{bmatrix} i_\alpha \\ i_\beta \end{bmatrix} \quad u = \begin{bmatrix} v_\alpha \\ v_\beta \end{bmatrix} \quad (14)$$

$$A = \begin{bmatrix} -\frac{R_s}{L_s} & 0 & -\frac{1}{L_s} & 0 \\ 0 & -\frac{R_s}{L_s} & 0 & -\frac{1}{L_s} \\ 0 & 0 & 0 & -\omega \\ 0 & 0 & \omega & 0 \end{bmatrix} \quad (15)$$

$$B = \begin{bmatrix} \frac{1}{L_s} & 0 \\ 0 & \frac{1}{L_s} \\ 0 & 0 \\ 0 & 0 \end{bmatrix} \quad (16)$$

$$C = \begin{bmatrix} 1 & 0 & 0 & 0 \\ 0 & 1 & 0 & 0 \end{bmatrix} \quad (17)$$

where i_x is the phase current in a two phase machine, v_x represents the phase to the neutral voltage in a two phase machine and e_x is the BEMF in a two phase machine. From (14), (15), (16) and (17), we applied state model in (18).

$$\frac{d}{dt}x = Ax + Bu \quad y = Cx \quad (18)$$

C. Angle/Speed of the Observer

The calculation of the phase can be done very simply through the trigonometric function atan2 . The function is fed by two components of the BEMF that mean $\alpha\beta$ parts in the stator reference frame. Function atan2 has handled the dangerous states in comparison to ordinary atan . Trigonometric function is problem for estimation of the speed because periodicity. Another problem of using this solution is the noise created when measuring the outputs from the BEMF observer. Complex filtering structures of the output are time-consuming. The timing is insignificant in non-real-time simulations but in real-time the feedback calculation becomes time critical.

For the estimation of speed it is better to use a phase locked loop (PLL). The PLL is a control system which generates the phase between the input signals. The PLL uses the PI controller in the same way as the BEMF observer, due to its gained error between the phases. The influence of noise of the BEMF signal in the angle and speed is reduced solely by the integrator in the PLL. PLL is illustrated in [8]. The principle is shown in Fig. 4.

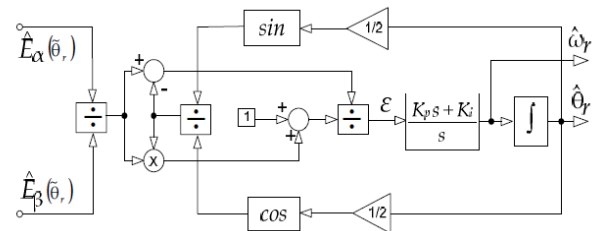


Fig. 4. Phase locked loop for the BEMF [8].

V. SIMULATION

The proposed techniques were simulated in the Matlab/Simulink as mentioned above. The two level control of the BLDC motor with the angle observer was simulated in accordance with the following diagram

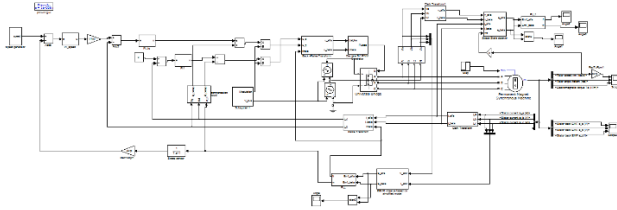


Fig. 5. Simulation diagram of the FOC with estimators.

The diagram contains several elements where the motor, inverter and the generator of the space vector modulation (SVM) are parts of the SimPowerSystems Toolbox. We used the BLDC motor with parameters as follows: $R_s = 18.7 \, \Omega$, $L_s = 1.365 \, \text{mH}$, $\lambda = 0.1717 \, \text{Vs}$, 1 pole pair and $J = 2.26 \times 10^{-5} \, \text{kgm}^2$. The inverter was built as a 3-phase universal bridge with the MOSFET technology. Other elements are the currents and the speed controller where we worked with a motor the bandwidth of which was equal to 8000 rad/s (including the inverter). The damping factor was 3.5 and the low-phase filter $\tau = 1.9894 \times 10^{-5} \, \text{s}$.

A. Unit Step with Sensor

The first simulation presents the FOC with sensors for the mechanical speed and the mechanical position of the rotor. We applied a load torque 3 Nm in time 0.1s. The input of the system was fed by speed value 3000 rpm. The following graph shows the view of the speed, position, current and torque of this measurement.

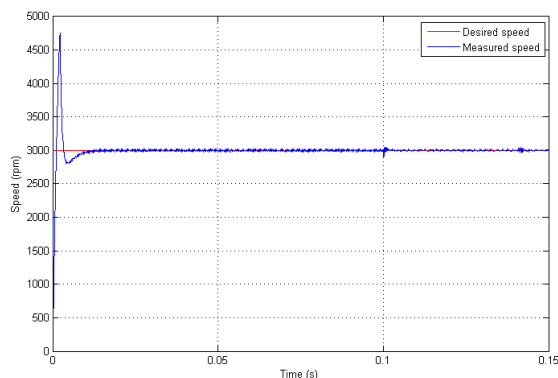


Fig. 6. Rotor speed with applied the unit step.

In the beginning, we gained a significant overshoot but later the speed stabilized. The controller handled the load without any problems. This can be seen zoomed in Fig. 7.

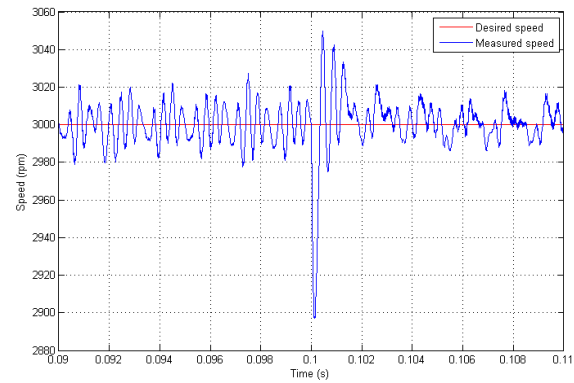


Fig. 7. Zoomed curve of the rotor speed with applied load.

B. Ramp with Sensor

We did not provide additional quantities to the input step but took a closer look at the speed when the motor starts along a ramp. The ramp slope had the value of 300 000. This means that the motor reached revolutions of 3000 rpm in 0.01 s time duration.

The motor was able to follow smoothly the desired ramp as shown in Fig. 8. It also confirms the progress of the position where it is satisfied with the S curve of the position in Fig. 9. Now we will look at the progress of the electromagnetic torque with the connected load.

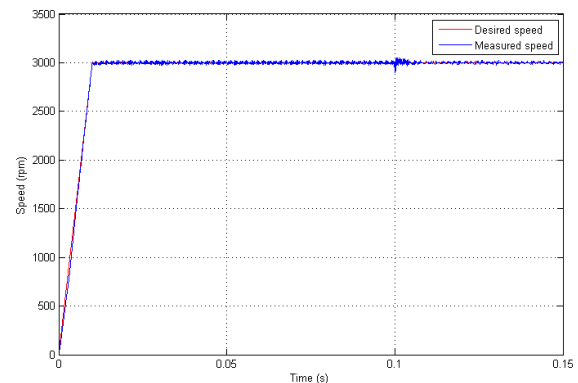


Fig. 8. Rotor speed with the applied ramp.

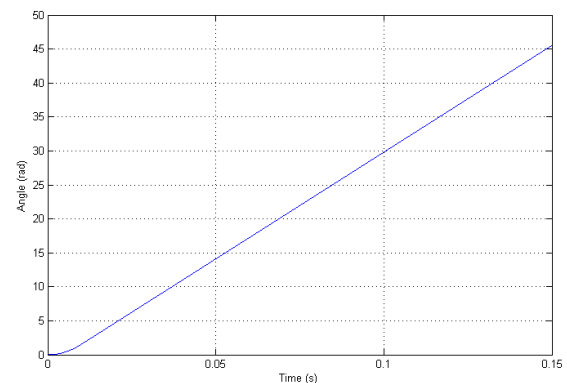


Fig. 9. Rotor position with the applied ramp.

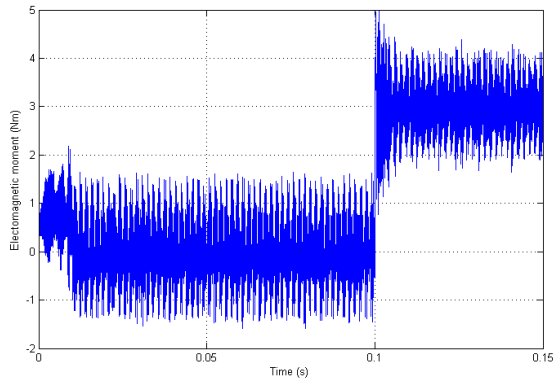


Fig. 10. Electromagnetic torque with the applied load from 0.1 s.

At the time moment of 0.1 second we can see the connected load, which increased the torque by 3 Nm.

C. Full Sensorless Control

In this section we measured the behaviour of the motor with the estimated rotor speed and position. For the estimation, the BEMF observer of the simplified model and the phase locked loop were used. In this case, we observed the shape of the diagrams of the rotor speed with and without load shown in Fig. 11.

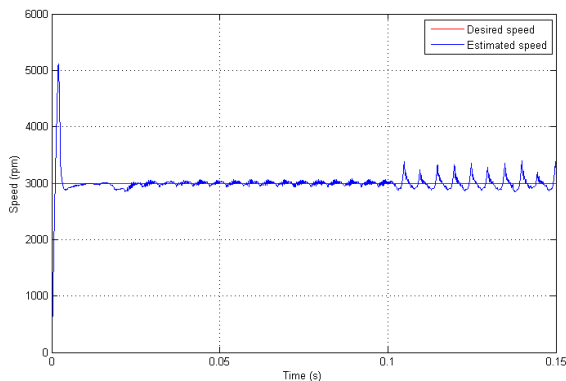


Fig. 11. The rotor speed with the sensorless control.

In the sensorless mode, the motor is capable of holding the level of the desired speed and is also capable of handling the disturbance of the load.

D. Comparison of Estimators

We continued with the full sensorless control from the previous section C. We compared the estimated speed (in only one case) and the rotor position with the measured values. Different types of estimators were compared.

The first estimator in order was the BEMF observer of the simplified model where we compared speed and position. It is shown in Fig. 12 and Fig. 13 that this estimator was the best of all our tested estimators, as it approximates the speed and the position of the rotor the most.

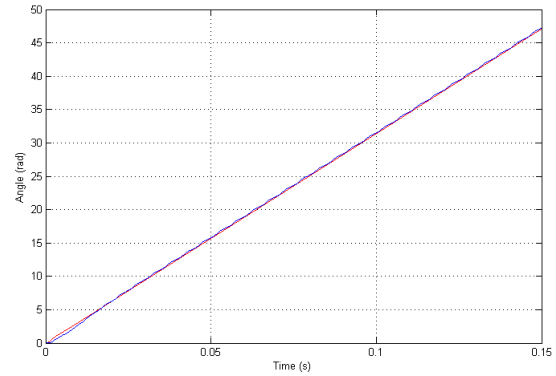


Fig. 12. Comparison of the rotor angle for the first estimator.

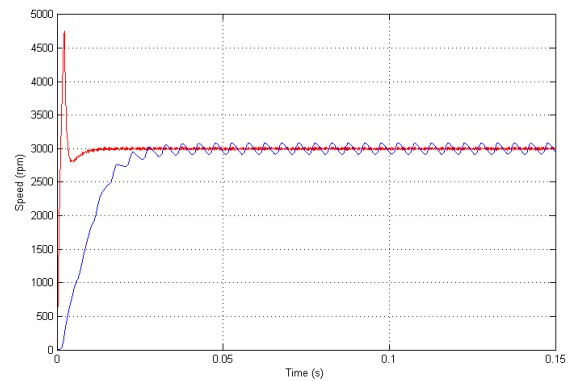


Fig. 13. Comparison of the rotor speed for the first estimator.

The second type of the estimator contains the previous type of the BEMF observer, however it contains trigonometric function atan2 for the phase elaboration.

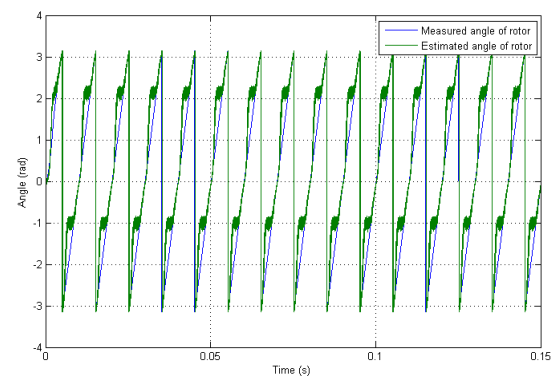


Fig. 14. Comparison of the rotor angle for the second estimator.

Regarding this estimator, we observed a ripple of the rotor angle. The angle was not integrated during the calculation but had a periodic cycle between $<-2\pi, 2\pi>$ rad. It was caused by the above mentioned periodicity of the trigonometric function. This shape of the rotor angle represents a problem for the speed estimation.

The third estimator with the state-space model with atan2 had the same problem as the second one. In addition, it had a phase shift with the real rotor angle as we can see in Fig. 15.

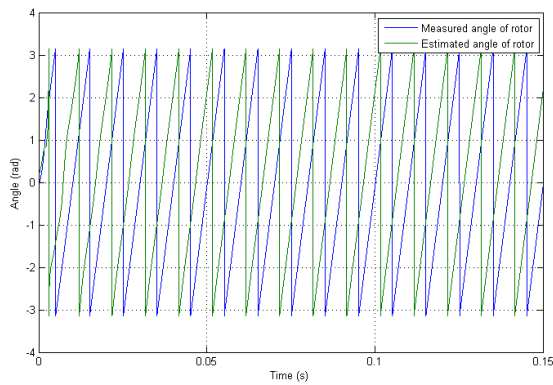


Fig. 15. Comparison of the rotor angle for the third estimator.

E. FOC and Six Step Commutation Differences

We take to the comparison FOC control and six-step commutation. From the Fig. 16 follows on that FOC control has a better behaviour of the dynamics when desired value of speed is following almost identical by FOC control value of speed.

Six-step commutation has a problem to keep the pace with the rapid increase of speed. This problem is associated with higher consumption of six-step commutation. The cause of lower efficacy in six-step control is hidden in principle of six-step control. It has not implementation of MTPA. Torque is not more stable during the operation than with FOC control but is crimped. The next reason of lower efficacy is hardware's format. It is several times the amount of transistor switching compared with FOC control.

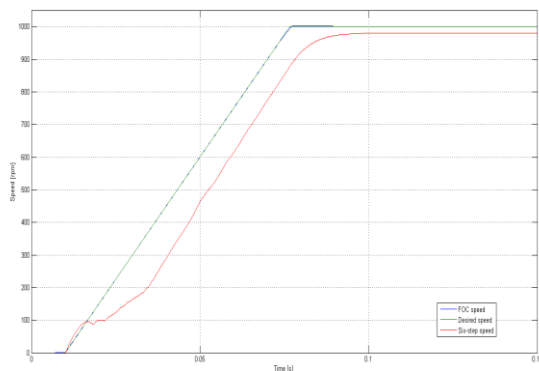


Fig. 16. The speed ramp with FOC and six-step.

VI. CONCLUSION

The aim of our study was to create a sensorless vector FOC of the BLDC motor. Our control contained current and speed loops which we could apply through the Park and Clark transformations. Thus, we gained a simulation model suitable for testing control through the Simulink Toolbox SimPowerSystems. After setting the control, we were looking for suitable candidates for the estimation of the position and speed of the rotor. The BEMF observer simplified motor model with PLL seemed to be appropriate, since sufficient precision at high speed provided the speed and the position of the rotor. We have understood that we have sufficiently applied the whole control on the simulation model of the motor and we can now proceed to its application to a real motor.

REFERENCES

- [1] Horizon Unmanned Systems (1.7.2015). Hycopter [online]. Available: <http://www.hus.sg/>
- [2] Atlantiksolar (1.7.2015). First fully-solar powered day/night flight achieved: In-air 28 hours without fuel! [onbratisla, vabrafaceline]. Available: <http://www.atlantiksolar.ethz.ch/>
- [3] Renesas (1.4.2010). Six Step Trapezoidal Control of a BLDC Motor Using Back-EMF [online]. Available: http://documentation.renesas.com/doc/products/mpumcu/apn/reu05b0073_r8cap.pdf
- [4] MathWorks (1.7.2015). Permanent Magnet Synchronous Machine [online]. Available: <http://www.mathworks.com/help/phymod/sps/powersys/ref/permanentmagnetsynchronousmachine.html>
- [5] Dave Wilson (4.3.2013). Teaching Your PI Controller to Behave (Part II) [online]. Available: <http://e2e.ti.com/blogs/b/motordrivecontrol/archive/2013/03/04/teaching-your-pi-controller-to-behave-part-ii>
- [6] Dave Wilson (9.3.2013). Teaching Your PI Controller to Behave (Part III) [online]. Available: <http://e2e.ti.com/blogs/b/motordrivecontrol/archive/2013/03/09/teaching-your-pi-controller-to-behave-part-iii>
- [7] Dave Wilson (14.3.2013). Teaching Your PI Controller to Behave (Part IV) [online]. Available: <http://e2e.ti.com/blogs/b/motordrivecontrol/archive/2013/03/14/teaching-your-pi-controller-to-behave-part-iv>
- [8] James Robert Mevey, Sensorless field oriented control of brushless permanent magnet synchronous motors. Kansas State University, Kansas, 2009.
- [9] C. Olivieri, M. Tursini, A novel PLL scheme for a sensorless PMSM drive overcoming common speed reversal problems. University of L'Aquila, Italy, 2012.
- [10] H. R. Mosaddegh, H. A. Zarchi, Maximum Torque per Ampere Control of Brushless Doubly Fed Induction Machine using Variable Structure Approach. Ferdowsi University of Mashhad, Iran, 2014.
- [11] Renesas (10.11.2015). InstaSPIN-FOC and InstaSPIN-MOTION. User's Guide. [online]. Available: <http://www.ti.com/lit/ug/spruhj1f/spruhj1f.pdf>